An integral approach to modeling PBL transports and clouds: EDMF @ ECMWF

Martin Köhler

ECMWF, Shinfield Park, Reading
RG2 9AX, United Kingdom
Martin.Koehler@ecmwf.int

1 Introduction

The importance of low clouds in terms of climate is illustrated by the fact that an additional 4% of low cloud cover would offset the radiative forcing resulting from CO_2 doubling (Randall et al., 1984). But land stratus, particularly during high pressure winter situations, can also provide a challenge to atmospheric models (Köhler, 2005). The improvement of stratocumulus and shallow convection in forecast and climate models has been the subject of a range of model developments by different groups (Lock et al., 2000; Lappen and Randall, 2001; Grenier and Bretherton, 2001; Bretherton et al., 2004). Here we summarise the path chosen at ECMWF to improve and unify the treatment of boundary layer clouds (Köhler 2005 or Tompkins et al. 2004 for more details).

A successful treatment of boundary layer clouds relies on realistic large scale conditions as well as sub-grid vertical transports and cloud generation and decay. In the ECMWF model four separate parametrizations that describe sub-grid physical processes interact to predict those clouds: vertical diffusion, convection, cloud and radiation. Because of the tight coupling between those physical processes inherent to boundary layer clouds it was decided to treat convective and diffusive transports within the PBL in one combined solver. Siebesma et al. (2007) provided such a framework with their Eddy-Diffusivity Mass-Flux (EDMF) method. This decomposition was derived by Siebesma and Cuijpers (1995), who showed that any vertical flux of a scalar quantity can be split into three contributions, the sub-core flux, the environmental flux and the mass-flux terms (see Fig 1):

$$\overline{w'\phi'} = a\overline{w'\phi_u'}^u + (1-a)\overline{w'\phi_e'}^e + a\overline{w}^u(\overline{\phi}^u - \overline{\phi}) \tag{1}$$

with

$$\begin{aligned}
\phi_u &= \phi_u' + \overline{\phi}^u \\
\phi_e &= \phi_e' + \overline{\phi}^e \\
\overline{\phi} &= a\overline{\phi}^u + (1-a)\overline{\phi}^e
\end{aligned}$$

The first two terms can then be approximated with a diffusion approach.

$$\overline{w'\phi'} = -K\frac{\partial\overline{\phi}}{\partial z} + M(\overline{\phi}^u - \overline{\phi}), \tag{2}$$

with $M = a\overline{w}^u$. This equation is integrated in a single solver. Note that this approach allows for any arbitrary setting of fraction a. This permits any mix of parametrizations using diffusion and mass-flux approaches where appropriate. Another advantage of the unification between parametrizations is numerical consistency

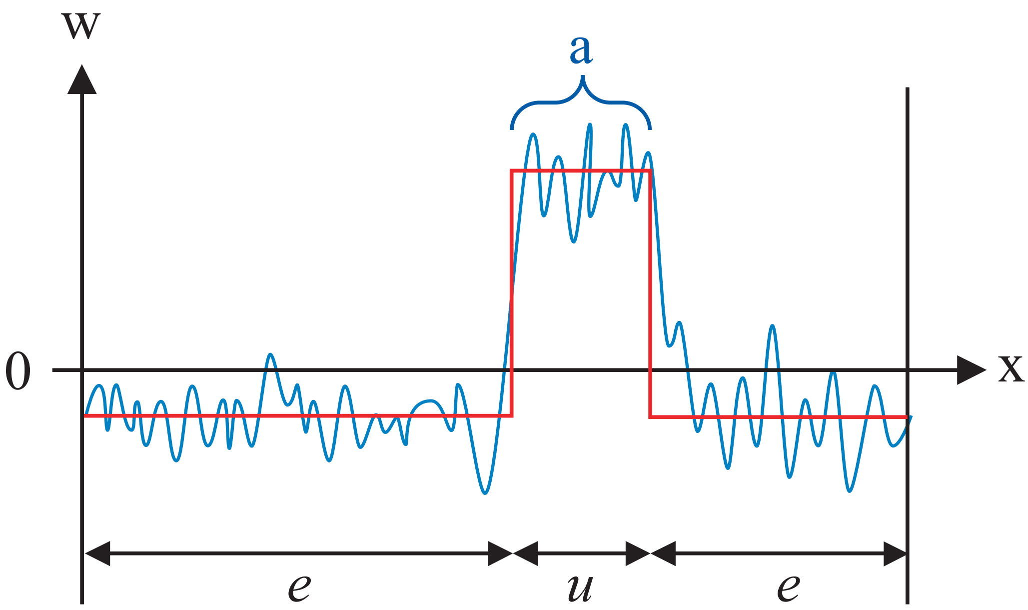

Figure 1: Two box decomposition of vertical velocity w between mass flux component (red line) and perturbations against the mean environment (e) and up-draught (u) (blue line). The perturbation components are being parametrised with a diffusion approach.

and simplicity. This EDMF approach can also easily be extended to include multiple mass-flux methods such as used in Arakawa and Schubert (1974) and Cheinet (2003).

$$\overline{w'\phi'} = -K\frac{\partial\overline{\phi}}{\partial z} + \sum_i M_i(\phi_{u,i} - \overline{\phi}) \tag{3}$$

Fig. 2 illustrates various applications of the EDMF framework for the ECMWF model. The top figure represents the parametrization of the dry convective PBL and plots the distribution function of w. A top fraction a is chosen to distinguish between the parts of the eddies that are described with the mass-flux and diffusion terms. Liquid water potential temperature θ_l and total water q_t are assumed to correlate with w. A similar approach is used for stratocumulus, where the effects of condensation have to be taken into account. Both those parametrizations are now operational in the ECMWF model. The full details of that implementation can be found in (Tompkins et al., 2004, chapter 5).

Two extensions of EDMF that employ the multiple mass-flux approach have been tested at ECMWF: (i) LES and observations have shown the importance of stratocumulus top forced down-draughts. They can be described by an additional mass-flux term as shown in the third panel of Fig. 2. This experimental setup is described in more detail below. (ii) For shallow convective parametrization Neggers et al. (2007) argue for the combination of a dry up-draught to cloud base and a cloudy up-draught to cloud top as appropriate.

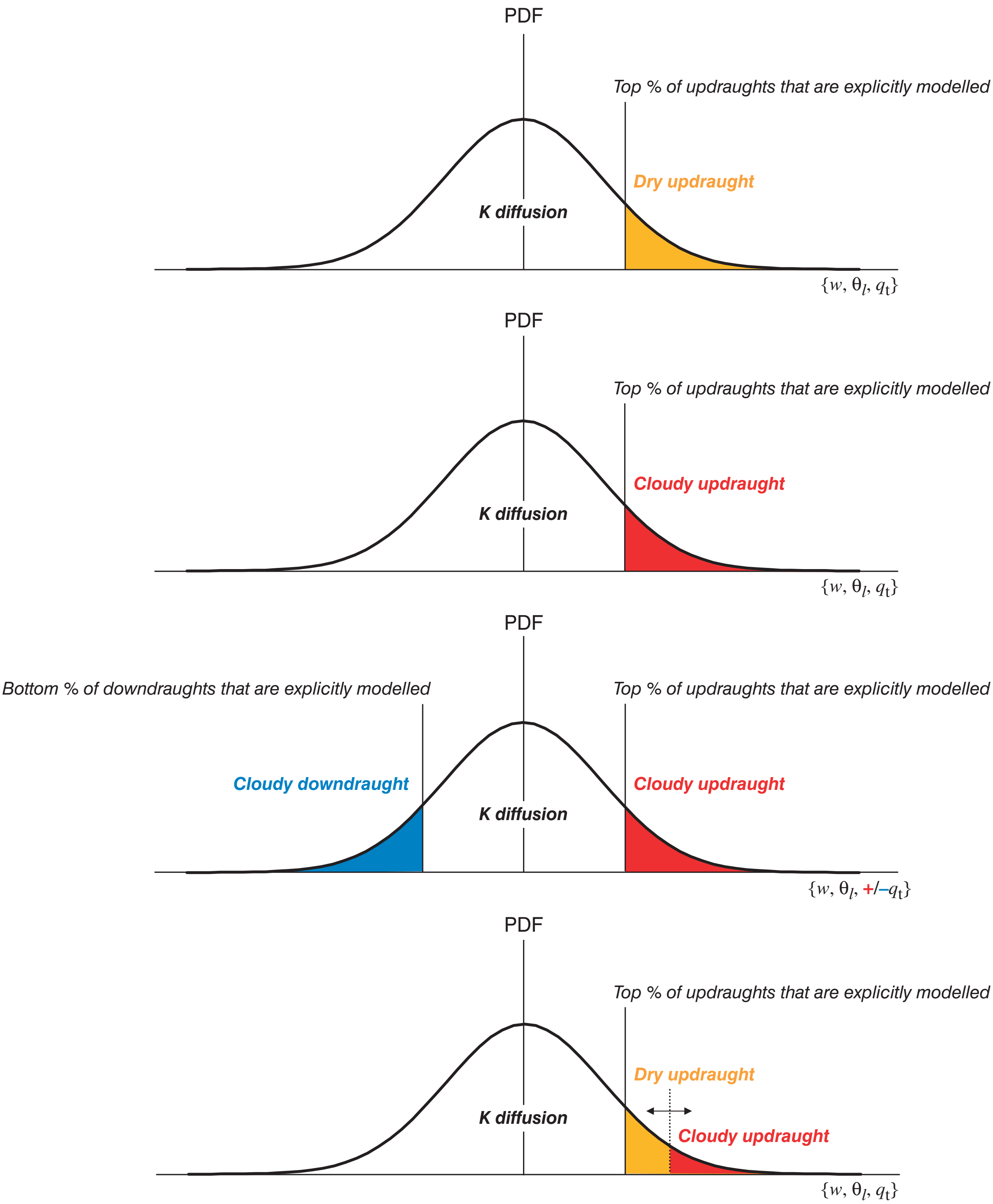

Figure 2: Statistical mass flux framework for organised eddies applied to the dry convective PBL, stratocumulus with up-draughts, stratocumulus with up- and down-draughts and shallow convection (top to bottom). See text for details.

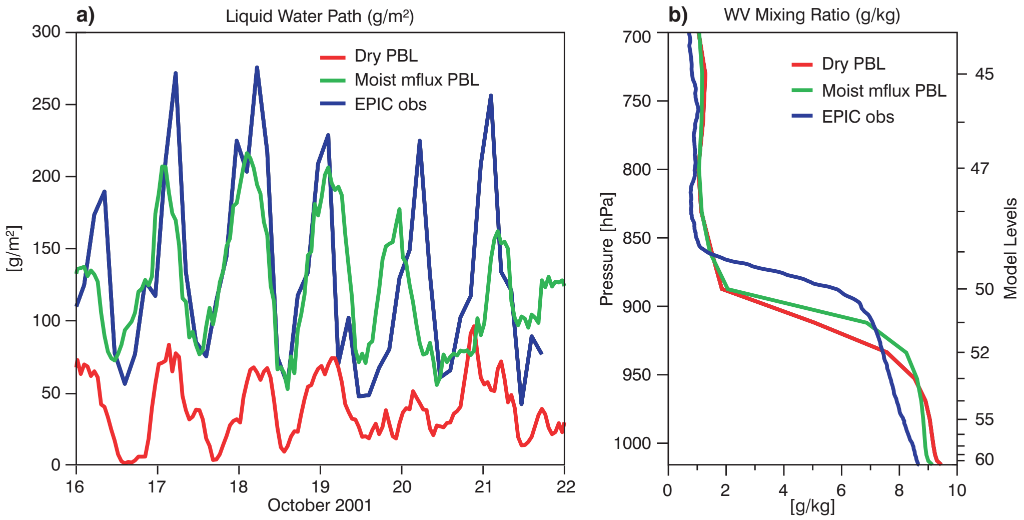

Figure 3: (a) Liquid water evolution during the Eastern Pacific Investigation of Climate (EPIC). It included a stationary observation period at 85°W, 20°S off the coast of Peru during 16-21 October 2001. The observed liquid water path is in blue. Results of the three-hourly forecasts using the old PBL scheme are in red and those using the new PBL scheme are in green. The day 1, 2 and 3 forecasts were averaged according to verifying time to obtain a smooth curve. (b) The corresponding profiles of water vapor.

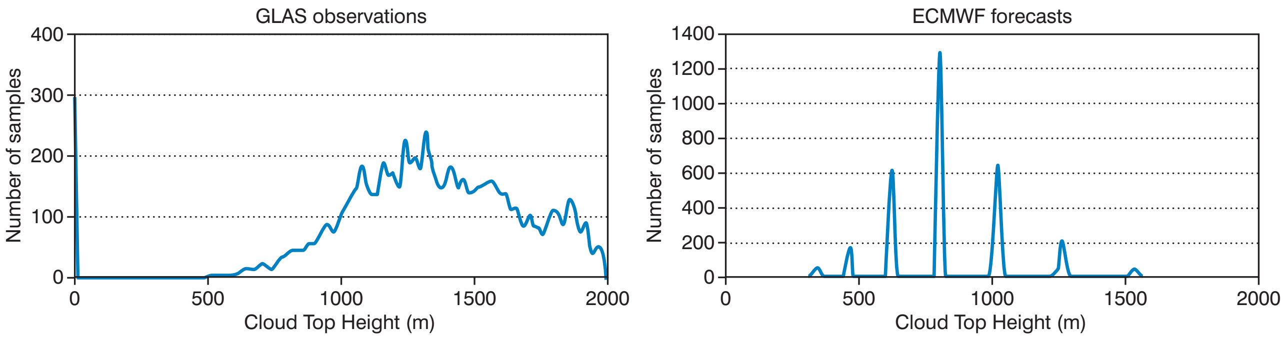

Figure 4: Stratocumulus top height as diagnosed by GLAS (Geoscience Laser Altimeter System) observations (left panel) and predicted by the ECMWF model (right panel). Courtesy of Maike Ahlgrimm, CSU.

2 Evaluation of the EDMF implementation for dry convective PBL and stratocumulus

The EDMF application to the dry convective PBL and stratocumulus was implemented in April 2005 in the ECMWF model. Substantial improvements to the prediction of marine low clouds as well as winter stratus were documented. As an example, we show results from a rerun of the full analysis/forecast system for the EPIC field experiment period in October 2001 off the coast of Peru (see Fig 3a). The new model not only increased the liquid water path (LWP) to realistic values. It also improved the diurnal cycle substantially including the burning of stratocumulus during day-time. Yet a too low PBL height by 1-2 layers (100-200m) has been diagnosed in a number of comparisons to observations. The profiles of moisture at the EPIC experiment are an example (Fig 3b). Together with Maike Ahlgrimm (CSU) we looked at GLAS cloud top height observations in stratocumulus regions and compared them to the model (Fig. 4). Again an under-prediction of

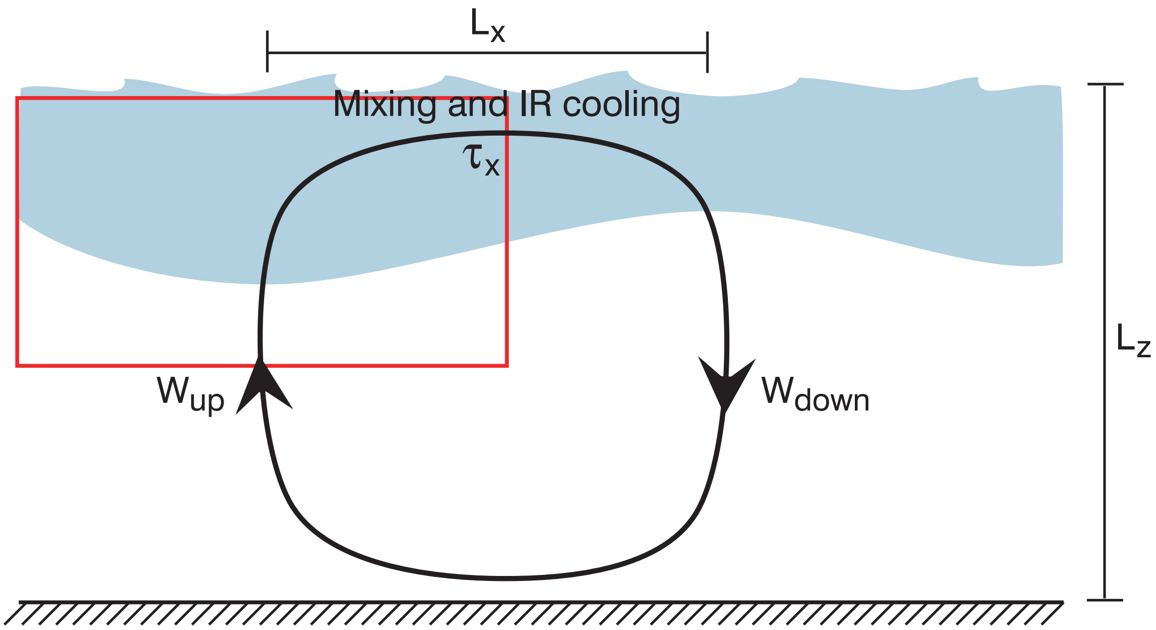

Figure 5: Schematic of up- and down-draughts w_{up} and w_{down} in the stratocumulus-topped boundary layer. L_x and L_z are the horizontal and vertical scales of the biggest eddies. τ_x is the time-scale a parcel in this cell spends near the cloud top. See text for explanation.

cloud top height by a few hundred meters can be seen. This problem is thought to be due to a too large parcel entrainment chosen as well as the numerics of the up-draught and the PBL top entrainment. Those issues are currently being addressed.

3 Stratocumulus up- and down-draughts

Turbulent fluxes in stratocumulus-topped boundary layers (STBL) are forced by buoyancy fluxes at the surface and the cloud top. Latter originates from the cooling due to radiative emission and is dominating the STBL forcing. Large eddy simulations and observations have demonstrated the relevance of down-draughts originating near cloud top to the STBL fluxes. It therefore makes sense to include those down-draught transports explicitly in the mass-flux component of our EDMF parametrization of stratocumulus. We start by describing the physics driving strong down-draughts from stratocumulus tops and make some scaling arguments. Consider a cell of depth PBL height L_z and width L_x (see Fig. 5). The time τ_x spent near the top of the cloud is approximately

$$\tau_x \sim \frac{L_x}{u} \sim \frac{L_z}{w_{up}} \sim 10^3 s, \tag{4}$$

with u the horizontal speed at cloud top and w_{up} the up-draught velocity. Continuity applied to the box in red is used ($L_x w_{up} = \frac{1}{2} L_z u + \frac{1}{2} L_z u$) to derive the second equality. Typical values $w_{up} = 1m/s$ and $L_z = 1000m$ are assumed. To estimate the radiative cooling of parcels near the cloud top we write

$$\triangle T_{rad} = \frac{\triangle R}{\rho c_p \triangle z_{rad}} \tau_x \sim 1K, \tag{5}$$

with R the radiative flux jump and $\triangle z_{rad}$ the depth of radiative cooling near cloud top. The approximate values $\rho = 1kg/m^3$, $\triangle z_{rad} = 100m$, $\triangle R = 100W/m^2$ and $\tau_x = 1000s$ were used to arrive at a 1K cooling of large

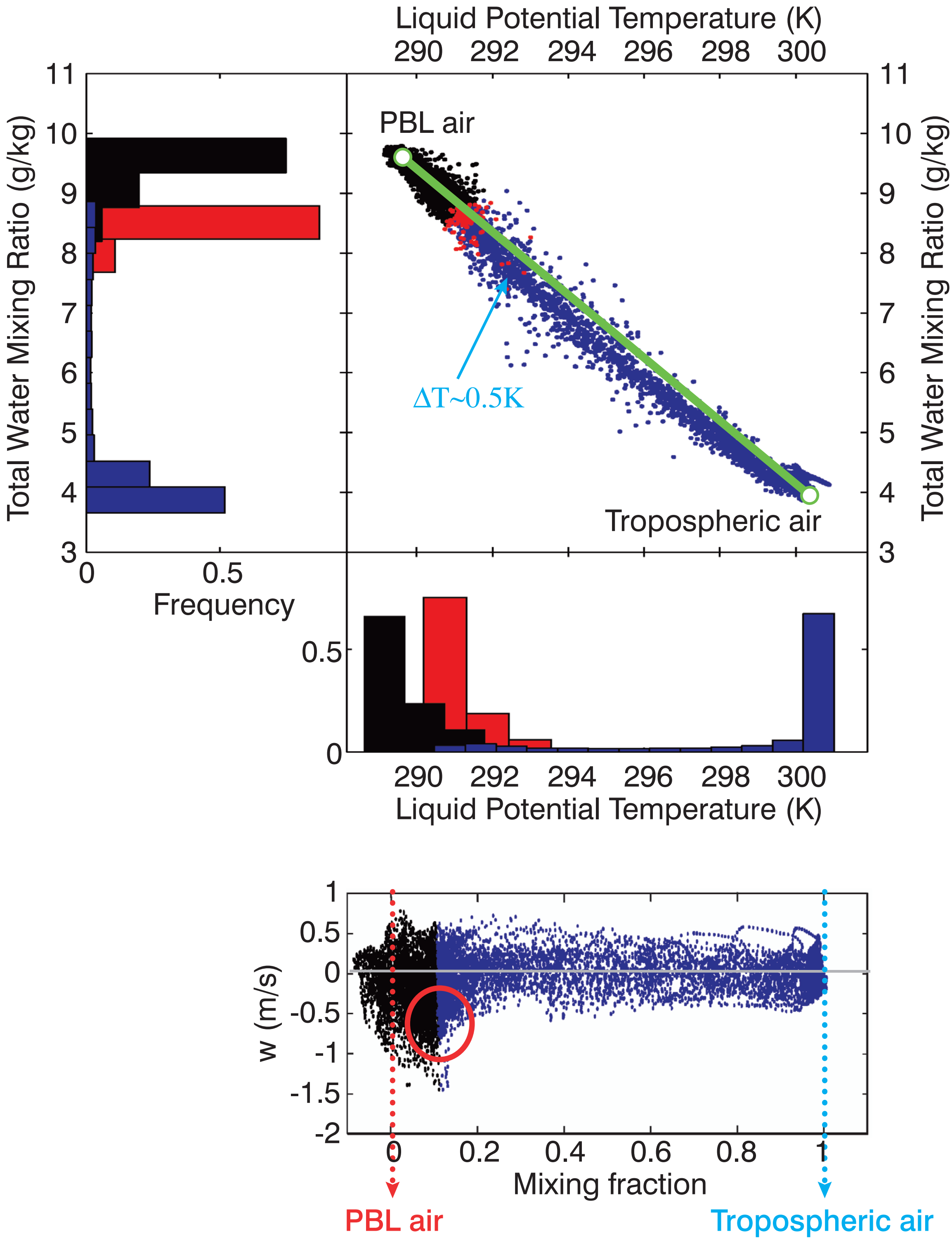

Figure 6: The top panel is a scatter plot of the conserved variables liquid water potential temperature θ_l vs. total water q_t for the DYCOMS-II case. Black, blue and red colours represent cloud, clear air and clear air samples adjacent to cloudy samples (edge samples) respectively. Frequency distributions of θ_l and q_t are shown along the two axis. The green line corresponds to the mixing line between PBL and tropospheric air parcels. The shift of pixels to the left (cold) therefore represents the impact of radiative cooling. The bottom panel plots the vertical velocity along the mixing line. Again black and blue corresponds to cloudy and clear pixels. Courtesy of Steve Krueger, Pete Bogenschutz and Mike Zulauf.

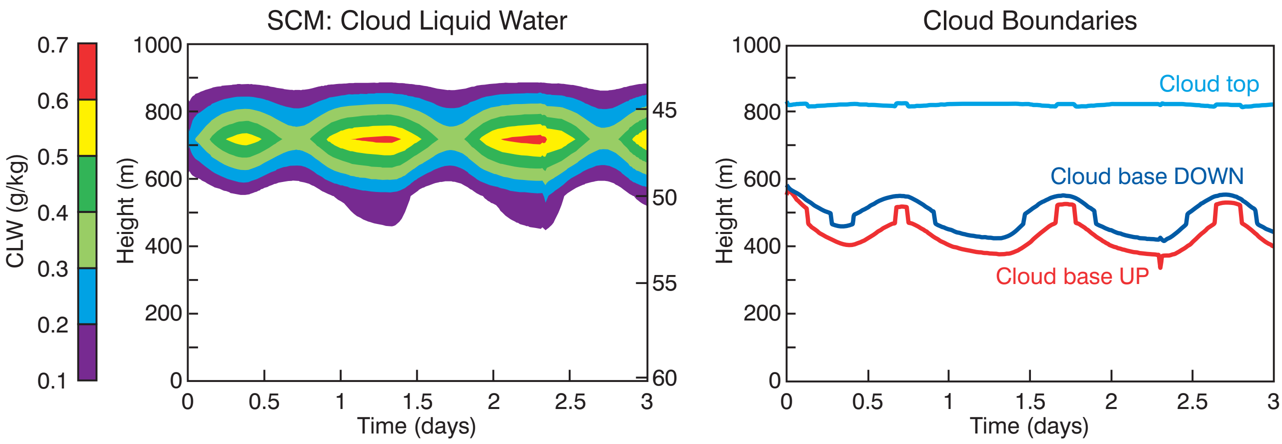

Figure 7: Results from a Single Column Model (SCM) using the ECMWF model modified to include stratocumulus down-draughts for the DYCOMS-II case. The left panel shows the evolution of cloud liquid water mixing ratio. The right panel shows the cloud base of up- and down-draughts as well as cloud top.

eddy parcels while they pass the cloud top. As comparison, the LES mixing line scatter plot for the DYCOMS II stratus field experiment (Fig. 6) indicates an approximate 0.5K radiative cooling of parcel just above cloud top. Next we define a vertical velocity scale relevant for cloud top forced turbulence

$$w^*_{top} = \left(\frac{g}{\theta_v}\overline{w'\theta_v'}^{top}L_z\right)^{1/3} \sim 1.5m/s \tag{6}$$

analogous to $w^* = \left(\frac{g}{\theta_v}\overline{w'\theta_v'}^{sfc}L_z\right)^{1/3}$. Here $\overline{w'\theta_v'}^{top} = \triangle R + \overline{w'\theta_v'}^{entr}$ is the buoyancy flux at the cloud top which includes radiative and entrainment parts. Taking the above mentioned estimates one arrives at a typical value of $w^*_{top} = 1.5m/s$. Note that the LES values of downward velocities are of the same magnitude (1m/s, Fig 6). To incorporate down-draughts in the mass-flux part of the EDMF framework requires the initialisation of the down-draught parcel in terms of vertical velocity, temperature and moisture. Motivated by the scaling arguments above we have chosen the following formulation

$$w_{down} = bw^*_{top} \tag{7}$$

$$\theta_{down} - \overline{\theta} = \theta_{exc} = b\frac{\overline{w'\theta'}^{top}}{w^*_{top}} = b\frac{\triangle R + \overline{w'\theta'}^{top,entr}}{w^*_{top}} \tag{8}$$

$$q_{t,down} - \overline{q_t} = q_{t,exc} = b\frac{\overline{w'q_t'}^{top}}{w^*_{top}} \tag{9}$$

Parcel entrainment is written as $\varepsilon = \frac{1}{\tau w_{down}}$. We have incorporated this stratocumulus down-draught parametrization into the current EDMF framework within the ECMWF single column model (SCM). Fig. 7 shows results from the identical DYCOMS II setup as the LES simulation mentioned here. The evolution of cloud water shows a realistic diurnal cycle with cloud base rising during daytime. The cloud base of the up-draughts are modelled about 50m lower than cloud base of the down-draughts. This is expected with the moisture effect dominating over the temperature/saturation mixing ratio effect. The LES simulation of this case shows a similar behaviour (Fig. 8) where the down-draughts (not shown) are at the location of the cloud break-up.

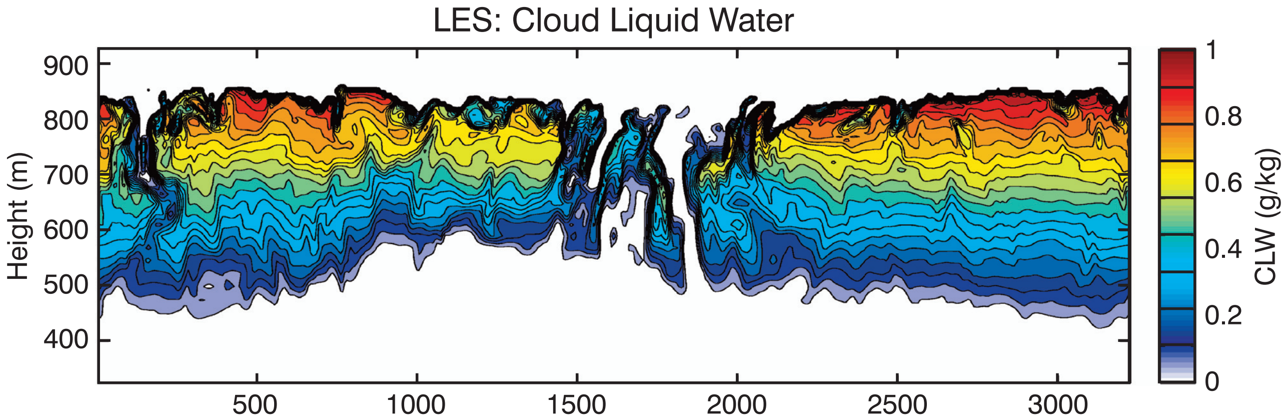

Figure 8: Snapshot of cloud water mixing ratio for an LES simulation running the DYCOMS-II case. Vertical resolution is 6m. Courtesy of Steve Krueger, Pete Bogenschutz and Mike Zulauf.

4 Summary and conclusions

We have given examples of how the EDMF framework can be adopted to the parametrization of various boundary layer regimes (e.g. dry PBL, stratocumulus and shallow convection). One could imagine this framework to be extended to include deep convection. A stronger coupling to clouds will also be beneficial.

The experimental extension to stratocumulus down-draughts proved technically simple. The first results are very encouraging. This formulation has the potential of improving the physical basis of our stratocumulus parametrization, improving their prediction and allowing for a better description of stratocumulus break-up.

Acknowledgements

We like to thank Steve Krueger and his group at the University of Utah for sharing his insight and material on the physics of stratocumulus top entrainment. His and other presentation at the GCSS meeting in Manhattan in September 2006 motivated the work on stratocumulus down-draughts. Maike Ahlgrimm (Colorado State University) is thanked for her PBL height analysis of the new ECMWF model, which motivated our work on parcel theory to solve the space lidar detected deficiencies. Anton Beljaars and Roel Neggers at ECMWF are thanked for their daily input in my work.

References

Arakawa, A. and W. H. Schubert, 1974: Interaction of a cumulus ensemble with the large-scale environment. Part 1, *J. Atmos. Sci.*, **31**, 674–701.

Bretherton, C. S., J. R. McCaa, and H. Grenier, 2004: A new parameterization for shallow cumulus convection and its application to marine subtropical cloud-topped boundary layers. Part I: Description and 1D results, *Mon. Wea. Rev.*, **132**, 864–882.

Cheinet, S., 2003: A multiple mass-flux parameterization for the surface generated convection. Part 1: Dry plumes, *J. Atmos. Sci.*, **60**, 2313–2327.

Grenier, H. and C. S. Bretherton, 2001: A moist PBL parametrization for large-scale models and its application to subtropical cloud-topped marine boundary layers, *Month. Weath. Rev.*, **129**, 357–377.

Köhler, 2005: Improved prediction of boundary layer clouds, *ECMWF Newsletter*, **104**, 18–22.

Lappen, C.-L. and D. A. Randall, 2001: Toward a Unified Parameterization of the Boundary Layer and Moist Convection. Part I: A New Type of Mass-Flux Model, *J. Atmos. Sci.*, **58**, 2021–2036.

Lock, A. P., A. R. Brown, M. R. Bush, G. M. Martin, and R. N. B. Smith, 2000: A new boundary layer mixing scheme. Part I: Scheme description and single-column model tests, *Mon. Wea. Rev.*, **128**, 3187–3199.

Neggers, R., A. Beljaars, and M. Köhler, 2007: A dual mass flux framework for boundary layer convection. Part I: Transport, *J. Atmos. Sci.*, submitted.

Randall, D. A., J. J. A. Coakley, C. W. Rairall, R. A. Kropfli, and D. H. Lenschow, 1984: Outlook for research on subtropical marine stratiform clouds, *Bull. Amer. Meteor. Soc.*, **65**, 1290–1301.

Siebesma, P. and J. W. M. Cuijpers, 1995: Evaluation of parametric assumptions for shallow cumulus convection, *J. Atmos. Sci.*, **52**, 650–666.

Siebesma, P., P. M. Soares, and J. Teixeira, 2007: An combined edddy diffusivity mass flux approach for parameterizing turbulent transport in the convective boundary layer, *J. Atmos. Sci.*, submitted.

Tompkins, A. M., P. Bechtold, A. Beljaars, A. Benedetti, S. Cheinet, M. Janisková, M. Köhler, P. Lopez, and J. Morcrette, 2004: Moist physical processes in the IFS: Progress and Plans, Technical Report 452, European Centre for Medium-Range Weather Forecasts, pp99.